research articles Journal of proteome research

Insertion of Membrane Proteins into Discoidal Membranes Using a Cell-Free Protein Expression Approach

Federico Katzen,[‡] Julia E. Fletcher,[‡] Jian-Ping Yang,[‡] Douglas Kang,[‡] Todd C. Peterson,[‡] Jenny A. Cappuccio,[†] Craig D. Blanchette,[†] Todd Sulchek,[†] Brett A. Chromy,[†] Paul D. Hoeprich,[†] Matthew A. Coleman,[†] and Wieslaw Kudlicki*[,‡]

Invitrogen Corporation, 5791 Van Allen Way, Carlsbad, California 92008, and Lawrence Livermore National Laboratory, 7000 East Avenue, Livermore, California 94551

Received April 9, 2008

We report a cell-free approach for expressing and inserting integral membrane proteins into water-soluble particles composed of discoidal apolipoprotein−lipid bilayers. Proteins are inserted into the particles, circumventing the need of extracting and reconstituting the product into membrane vesicles. Moreover, the planar nature of the membrane support makes the protein freely accessible from both sides of the lipid bilayer. Complexes are successfully purified by means of the apoplipoprotein component or by the carrier protein. The method significantly enhances the solubility of a variety of membrane proteins with different functional roles and topologies. Analytical assays for a subset of model membrane proteins indicate that proteins are correctly folded and active. The approach provides a platform amenable to high-throughput structural and functional characterization of a variety of traditionally intractable drug targets.

Keywords: Membrane protein • nanodisc • proteomics • cell-free • protein expression

Introduction

Integral membrane proteins (MPs) comprise nearly 30% of any given proteome, play fundamental roles in transport, signaling, bioenergetics, and cell-growth processes, and account for over 50% of all human drug targets. However, biochemical and structural characterization of membrane bound proteins is currently cumbersome, often intractable, and lags far behind the study of water soluble proteins. Overexpression of MPs *in vivo* frequently results in cell toxicity, protein aggregation, misfolding, and low yield. Membrane protein purification involves detergent extraction, detergent refolding, or reconstitution into liposomes, processes that inexorably lead to constraints on protein accessibility, surface immobilization, and activity assays.[1]

A novel method for displaying active MPs in nanoscale particles made of lipoprotein encircled membrane bilayers has been described.[2] These particles are referred to as nanodiscs[3] or nanolipoprotein particles (NLPs).[4] NLPs are self-assembled discoidal particles composed of a planar phospholipid membrane bilayer surrounded by an apolipoprotein ring (scaffold protein). Advantages of NLPs include water-solubility, monodispersity within preparations, consistency between preparations, flexible lipid composition, and more importantly, unrestricted and simultaneous access to both faces of the membrane leaflet.[5] It has been demonstrated that certain MPs can be incorporated into NLPs by adding detergent solubilized MPs to the NLP assembly process.[6] Despite the demonstrated capture of MPs in NLPs, the current method to produce NLP-associated MPs is laborious and requires successful expression, purification, and solubilization of MPs, many of which exhibit detrimental idiosyncratic behaviors in the course of one or more of these procedures, prior to assembly with NLPs. Here, we report a simple approach to assemble MPs directly into NLPs by introducing preformed empty NLPs into cell-free membrane protein expression reactions.

Experimental Section

Plasmids and Clones. Unless otherwise specified, genes encoding MPs (Gateway compatible Ultimate ORF collection, Invitrogen, Carlsbad, CA) were recombined into the plasmid pEXP4-DEST (Invitrogen, Carlsbad, CA) following the manufacturer's directions. The gene encoding EmrE from *Escherichia coli* (GenBank acc. no. Z11877) was PCR-amplified using primers 5′-GGGGACAAGTTTGTACAAAAAAGCAGGCTTCATGAACCCTTATATTTATC-3′ and 5′-GGGGACCACTTTGTACAAGAAAGCTGGGTCTTAATGTGGTGTGCTTCG-3′ and recombined via BP and LR Gateway reactions (Invitrogen, Carlsbad, CA) into pEXP6-DEST, a modified pEXP3-DEST plasmid (Invitrogen, Carlsbad, CA) devoid of the histidine tag coding sequence. Also, the exact EmrE coding sequence (GenBank acc. no. Z11877) was PCR-amplified and cloned into pEXP5-NT/TOPO (Invitrogen, Carlsbad, CA). Human apoA1 (GenBank acc. no. NM_000039) was PCR-amplified using primers 5′-CACGTGGATGAACCACCACAAAG-3′ and 5′-CCTAGGCTATTGAGTGTTCAGTTTTTTGG-3′, codon-optimized, and cloned into pET302NT-

* To whom correspondence should be addressed. Dr. Wieslaw Kudlick, Invitrogen Corp., 5791 Van Allen Way, Carlsbad, CA 92008. E-mail: toni.kudlicki@invitrogen.com.
‡ Invitrogen Corp.
† Lawrence Livermore National Laboratory.

10.1021/pr800265f CCC: $40.75
Published on Web 06/17/2008

His (Invitrogen, Carslbad, CA) between the *Pml*I and *Avr*II restriction sites. The bacteriorhodopsin (bR) gene sequence was PCR-amplified from plasmid p72bop[7] using primers 5′-GGGGCATATGCAAGCTCAAAT-3′ and 5′-GGGGATC-CAAAAAAAAACGGGCC-3′. The resulting PCR product was cloned into pIVEX 2.4b (Roche Applied Science, Indianapolis, IN) using the *Nde*I and *Bam*HI restriction enzyme sites (pIVEX 2.4b-bR). The plasmid (pET32-E4NT) and expression conditions to produce the N-terminal 22 kDa fragment of human apolipoprotein E4 (apoE422K) were described earlier.[8] The sequence of the GFP gene (acc. no. U62637) was PCR-amplified and cloned into pENTR/D-TOPO (Invitrogen, Carlsbad, CA). The resulting plasmid was digested with *Nhe*I and *Pvu*II, and the released DNA fragment was cloned into a pUC18-derivative between the T7 promoter and T7 terminator elements (pFKI032).

NLP Samples and Lipids. Phospholipids were from Avanti Polar Lipids (Alabaster, AL). NLPs composed of mature human apoA1 and 1,2-dimyristoyl-*sn*-glycero-3-phosphocholine (DMPC) were made using an established protocol with minor modifications.[3] Briefly, DMPC, cholate, and apoA1 were mixed in a molar ratio of 140:280:1 and subjected to 3 temperature shift cycles (RT for 10 min and 30 °C for 10 min). The mix was incubated further for 90 min and the detergent was removed with Bio-Beads SM-2 nonpolar polystyrene adsorbents (Bio-Rad, Hercules, CA) following the manufacturer's directions. Monodisperse NLPs were recovered using size exclusion chromatography (Superdex 200 10/300 GL, GE Healthcare, Uppsala, Sweden). NLPs composed of his-apoE422K and DMPC were made as described.[4] Briefly, the apolipoprotein and lipids were combined in a mass ratio of 4:1 in TBS buffer and subjected to 3 temperature shift cycles (30 and 20 °C) with a final overnight incubation at 23.8 °C. NLPs were purified with size exclusion chromatography (Superdex 200 10/300 GL, GE Healthcare, Uppsala, Sweden).

Cell-Free Protein Expression Reactions. *E. coli*-based cell-free protein expression reactions were set up using Expressway Maxi Cell-Free *E. coli* Expression System (Invitrogen, Carlsbad, CA) following the manufacturer's directions. NLPs were added to the reactions at a final concentration of 1.35 mg/mL. Where indicated, [^{35}S]Met (135 mCi/mmol final) (Perkin-Elmer, Waltham, MA) was added and yield was calculated by TCA precipitation following the manufacturer's directions. The soluble fraction from the reactions was obtained by centrifugation at 14 000*g* for 5 min. Autoradiograms were generated by overnight exposures. Where indicated, all trans-retinal (Sigma, St. Louis, MO) was added at a final concentration of 5 μM. Eukaryotic-based cell-free protein expression reactions were set up using TNT-coupled rabbit reticulocyte lysate (Promega, Madison, WI) and RTS 100 Wheat Germ CECF (Roche Applied Science, Mannheim, Germany) kits following the manufacturer's directions. NLPs were added to the reactions at a final concentration of 0.27 mg/mL. Final specific activity for [^{35}S]Met was 81600 and 91 mCi/mmol for the rabbit reticulocyte and wheat germ systems, respectively.

Protein Analysis. Proteins were purified using the Ni-NTA Purification System (Invitrogen, Carlsbad, CA) following the manufacturer's directions. In-gel visualization of proteins in denaturing gels was performed by Coomassie-blue staining or by using the Lumio Green Detection Kit (Invitrogen, Carlsbad, CA) and subjecting the gel to laser scanning (Typhoon 8600 Variable Mode Imager, GE Healthcare, Piscataway, NJ). Native gel electrophoresis was performed on 4−12% Tris-glycine polyacrylamide gels (Invitrogen, Carlsbad, CA) using NativePAGE running buffer (Invitrogen, Carlsbad, CA). Proteins were visualized with Sypro Ruby protein gel stain (Bio-Rad, Hercules, CA). Absorbance spectra of bR were collected in a Ultrospec 5300 pro UV/Visible spectrophotometer (Amersham Biosciences). Protein and NLP concentration were determined using the BCA Protein Assay Kit (Pierce, Rockford, IL).

EmrE Activity Assays. EmrE activity was assayed using a tetraphenylphosphonium (TPP^+)-binding assay.[9] Briefly, EmrE was expressed *in vitro* as described above and immobilized on Ni^{2+}-nitrilotriacetic acid beads (Probond Protein Purification System; Invitrogen, Carlsbad, CA). The beads were then washed with binding buffer containing 150 mM NaCl, 10 mM imidazole, and 15 mM Tris·Cl, pH 7.5, and the protein content was estimated by gel densitometry. One tenth of a microgram of EmrE was added to the binding buffer containing 0.125−320 nM [^{3}H]TPP^+ (28 Ci/mmol; GE Healthcare), and incubated for 1 h at room temperature. Nonspecific binding was determined by competition with 20 μM cold TPP^+ (Sigma-Aldrich, St. Louis, MO). Data points were fitted to a saturation binding curve by nonlinear regression using Prism (GraphPad Software, San Diego, CA).

Atomic Force Microscopy (AFM). Atomically flat mica disks were glued to metal substrates to secure them to the scanner of a stand-alone MFP-3D AFM instrument (Asylum Research, Santa Barbara, CA). The AFM has a closed loop in the *x*, *y*, and *z* axes. The topographical images were obtained with Biolevers (Olympus, Tokyo, Japan) with a spring constant of 0.03 N/m. Images were taken in alternate contact (AC) mode in liquid, with very low amplitudes at the primary resonance frequency that was obtained from thermal analysis of the cantilever in solution. Height, amplitude, and phase images were recorded. Heights of contiguous particles in images were determined by cross-sectional analysis in the slow scan direction, using IgorPro software routines (WaveMetrics, Portland, OR). The maximum particle height was recorded and the results were displayed by histogram analysis. Experiments were carried out in a temperature controlled room at 23 ± 1 °C. The thermal spectrum of the cantilevers was obtained both in air and liquid, and the stiffness was estimated by fitting with the thermal noise theory and compared to the Sader method for the normal spring constant of a rectangular cantilever.[10] The error in calculating the spring constant is estimated to be <20%.

Size Exclusion Chromatography (SEC). SEC was conducted using a Shimadzu VP HPLC device (Columbia, MD) using a Superdex 200 10/300 GL column (GE Healthcare, Uppsala, Sweden), in TBS at a flow rate of 0.5 mL/min. The column was calibrated with four protein standards (thyroglobulin, ferritin, aldolase, and chymotrypsinogen) of known molecular weight and stokes diameter that span the separation range of the column and the NLP samples. The void volume was established with blue dextran. When indicated, samples were previously concentrated through a Vivaspin 100 kDa polyethersulfone membrane (Sartorious, Edgewood, NY).

Results

Two Strategies for Complex Formation and Purification. In initial experiments, we used the *E. coli* multidrug transporter EmrE (GenBank acc no. Z11877), a protein that has been extensively studied and is known to express at relatively high rates in cell-free protein expression systems.[11] For these experiments, the scaffold proteins (apoA1 or apoE422K) in the preformed NLPs were affinity-tagged for purification, whereas

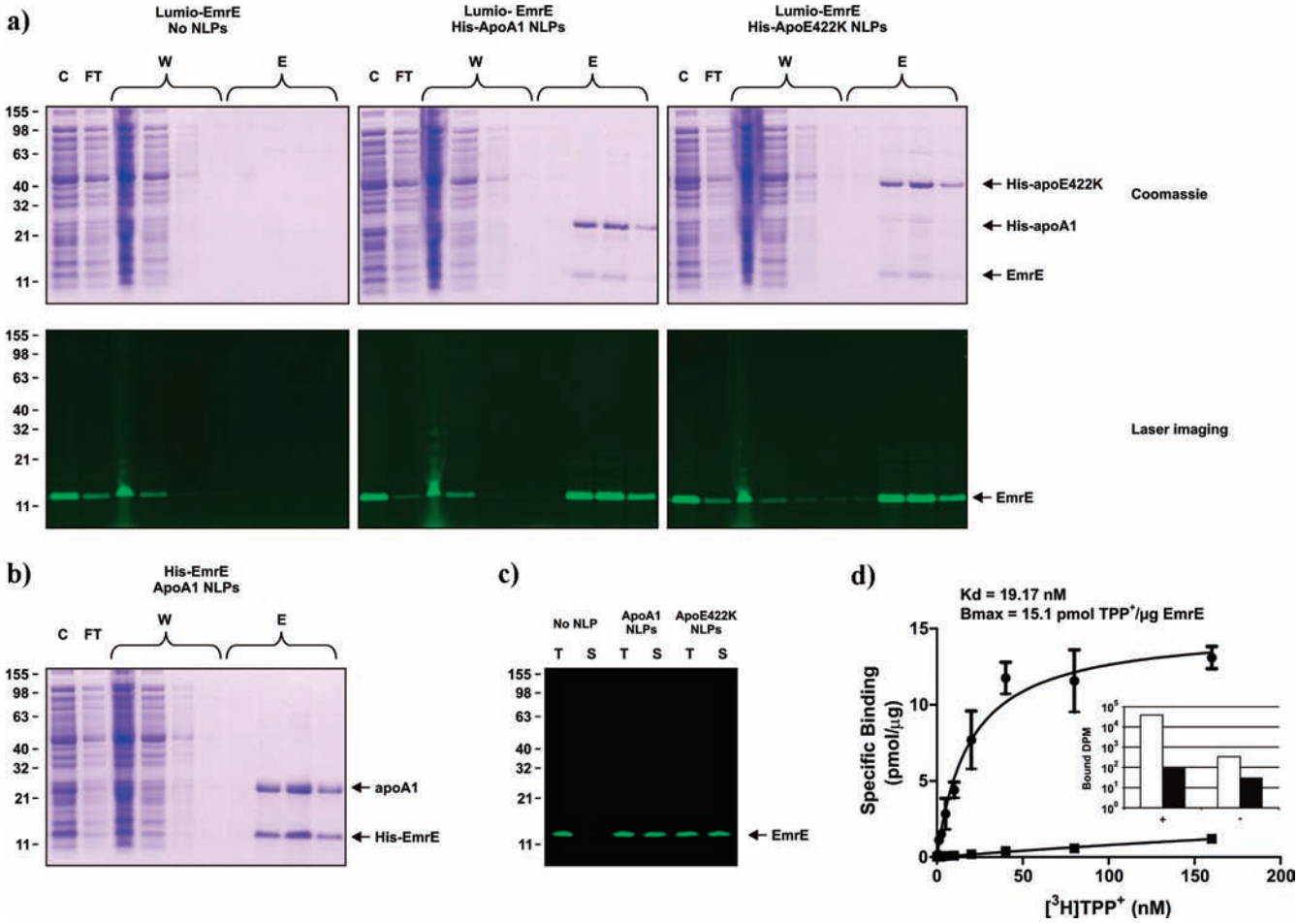

Figure 1. *In situ* complex formation between NLPs and EmrE. (a) *E. coli* EmrE was expressed *in vitro* either in the absence or presence of NLPs. NLPs were composed of histidine-tagged apoA1 (his-apoA1) as a scaffold and DMPC, or histidine-tagged apoE422K (his-apoE422K) and DMPC. Proteins were separated by SDS electrophoresis and stained by Coomassie blue or visualized by laser scan imaging. EmrE was fused to a Lumio recognition sequence (Cys-Cys-Pro-Gly-Cys-Cys)[37] and lacked a histidine tag. (b) Reactions were set up and processed as in panel a. NLPs were composed of apoA1 devoid of any additional sequence and DMPC. EmrE was fused to a histidine tag. (c) Proteins from the total crude extract and from the soluble fraction in panel a were separated by SDS-electrophoresis and visualized by laser scan imaging. (d) $[^3H]TPP^+$ binding analyses were performed in triplicate as described[9] (filled circles). Unspecific binding (filled squares) was determined by assessing $[^3H]TPP^+$ bound in the presence of 20 μM nonradioactive competitor. The DNA source for EmrE was pEXP5-NT-EmrE. In the inset, $[^3H]TPP^+$ binding was performed in the absence (empty bars) or presence (filled bars) of nonradioactive TPP^+. Binding reactions were carried out with EmrE synthesized in the presence (+) or absence (-) of NLPs. NLPs were composed of apoA1 devoid of any additional sequence and DMPC. C, crude extract; FT, flow-through fraction; W, wash fractions; E, imidazole-eluted fractions, T, total crude extract; S, supernatant.

EmrE was expressed with a lumio recognition sequence (Cys-Cys-Pro-Gly-Cys-Cys) but devoid of a poly-histidine tag. The opposite strategy, where the affinity-tagged protein was EmrE, was also followed. Under our conditions, EmrE expressed at levels up to 0.4 mg/mL of reaction. In all these cases, results showed that EmrE produced by the cell-free methodology readily copurified with the NLPs, suggesting that complexes were formed between NLPs and EmrE (Figure 1a,b). In addition, a strong correlation between complex formation and protein solubility was found (compare panels a and c of Figure 1). Finally, activity assays showed that the EmrE substrate $[^3H]$tetraphenylphosphonim (TPP^+) binds specifically to EmrE only when NLPs are included in the reaction (Figure 1d, inset). Earlier kinetics measurements of EmrE based on $[^3H]TPP^+$ binding were conducted in the presence of a variety of detergents such as *N*-dodecyl-b-D-maltoside, *N*-octyl-β-D-glucopyranoside and SDS.[12–15] In those circumstances, K_d values ranging from 2.6 to 45 nM were reported.[12–15] $[^3H]TPP^+$ binding using EmrE preparations reconstituted into unilamellar vesicles could not be determined.[13] In our case, we determined the binding constants of EmrE complexed with NLPs in the absence of detergents finding that the binding to $[^3H]TPP^+$ is saturable at a value of 15.1 pmol ligand/μg EmrE with a K_d of 19.17 nM (Figure 1d). Overall, our results indicate that EmrE is active, suggesting that it is correctly folded, therefore, correctly inserted into the NLPs' lipid bilayer.

Analytical Characterization of the Complexes. To further study the biochemical and biophysical properties of MP-NLP complexes, *Halobacterium salinarum* bacteriorhodopsin (bR) (GenBank acc. no. J02755) was used as a second model system. Twice as large as EmrE, bR allowed us to readily distinguish between empty and loaded NLPs when using a variety of biochemical and biophysical methods (see below).

The bR protein is a 7 transmembrane, α-helix, light-driven proton pump with a cofactor pocket in which a retinal molecule is covalently linked. Although its mechanism does not involve

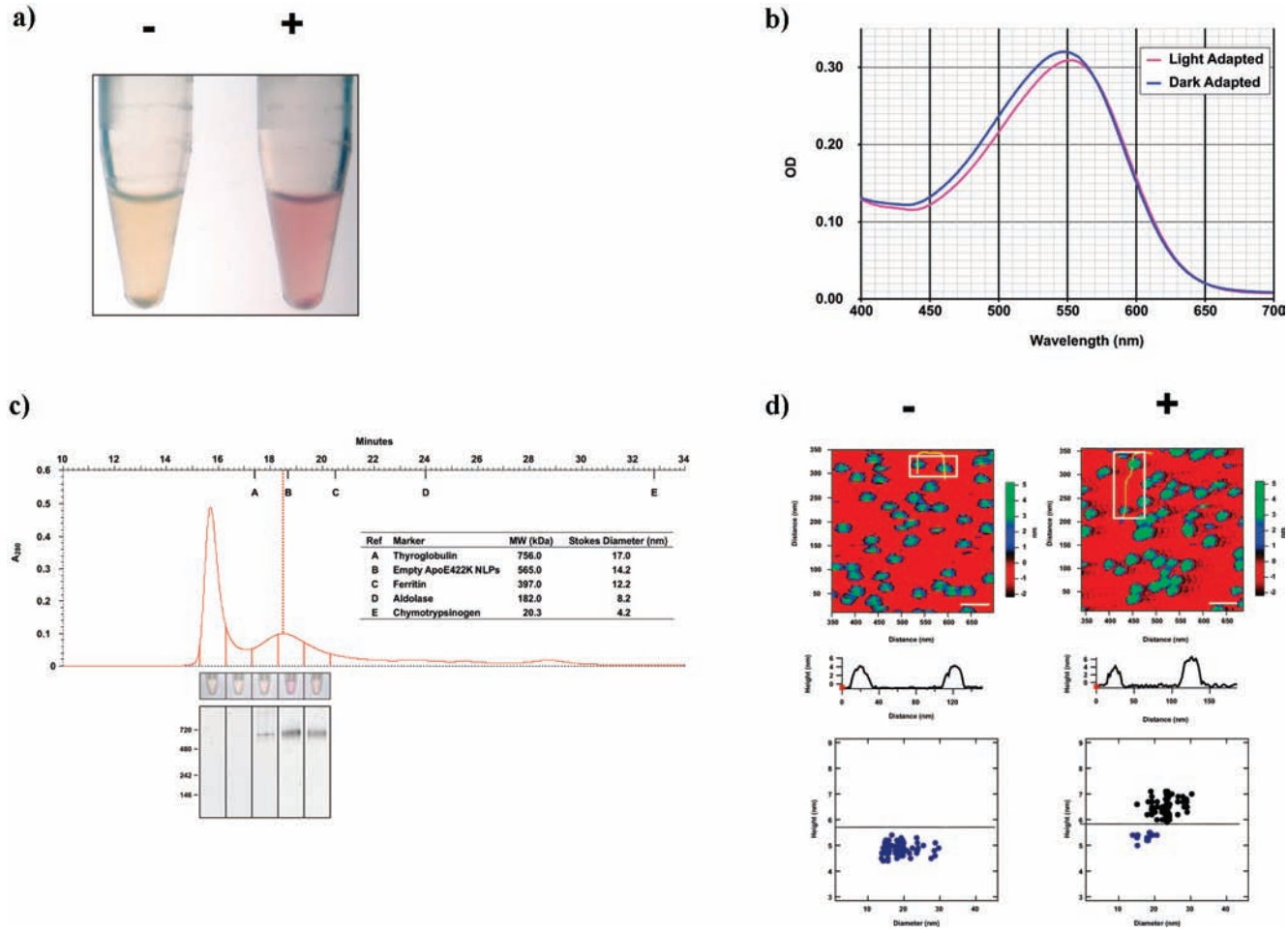

Figure 2. Formation and characterization of NLP-bR complexes. (a) Photograph of the reaction tubes where bR was expressed in the presence (+) or absence (-) of NLPs. NLPs were composed of histidine-tagged apoE422K as a scaffold and DMPC. (b) NLP-bR complexes were purified over a nickel column and samples were light-adapted (white light for 15 min) or kept in the dark for 4 h. (c) To remove small particles, purified complexes were concentrated through a 100 kDa cutoff membrane and run over a precalibrated Superdex 200 10/300 GL column. Elution times and biophysical properties of the markers are indicated. Photograph of the tubes of relevant fractions are depicted. Aliquots of those fractions were run on a native gel and results are shown. MW markers are indicated on the left. (d) Panels show 350 × 350 nm topographical AFM images of empty (-) and bR-loaded (+) his-apoE422K-NLP complexes obtained in panel c. Scale bar, 50 nm. A color bar scale identifies NLP height. A section line trace below the two panels shows a cross section of the height of the particles identified in the insets above. The average height for empty and bR-loaded NLPs is 4.9 ± 0.2 and 6.5 ± 0.3 nm, respectively. The bottom panels represent scatter plots of NLP diameter and height of the corresponding panels above. The purpose of AFM studies is to assess particle height only, as the diameter size obtained by AFM is known to show a low *x*, *y* resolution due to tip convolution effects.

the activation of G proteins, bR has been used as structural model for rhodopsin and other GPCR family members.[16] A purple color and characteristic absorption peaks at 558 and 568 nm (trimer) or at 546 and 553 nm (monomer) indicate a correctly folded, functional bR,[17] and that the retinal is bound to a Lys residue at position 216 via Schiff base formation.[18,19]

Early reports showed that bR was inactive when synthesized *in vitro*, but could be functionally refolded using halobacterial lipids.[19,20] More recently, it was shown that active bR could be produced *in vitro*; however, a limited fraction of the translated material could be incorporated into the membranes.[21]

With *in vitro* synthesis of bR in the presence of preformed, naked NLPs, the characteristic purple color could be observed as early as 5 min after initiation of the reaction (Figure 2a). This effect was accompanied by a dramatic increase in protein solubility (nearly 100%) compared to the case where no NLPs were added and could be observed using NLPs of different size and composition (see Further Validation of the Approach below). Under our conditions, bR expressed at levels up to 0.9 mg/mL of the reaction. The assays were performed using NLPs composed of nontagged apoE422K, which are significantly larger in size than NLPs composed of apoA1. The resulting bR-NLP complexes were purified by nickel affinity using the N-terminal histidine tag attached to bR. Spectral analyses of the corresponding purified complexes, either exposed to light or incubated in the dark, exhibited the characteristic bR peaks yielding a 5 nm shift, which indicates that the majority of the bR was in a monomeric form[17] (Figure 2b). This result is in agreement with other studies that used preformed apolipoprotein scaffolds to solubilize native forms of bR.[22]

To determine the molecular weight (MW) and stokes diameter of the bR-NLP complexes, affinity-purified samples were fractionated using SEC (Table 1, Figure 2c). Size and width differences found between empty and NLPs thought to contain bR are consistent with models where one to three molecules of bR are inserted into each NLP. Note that three bR molecules

Table 1. Physical Characterization of Complexes

type of NLP particle	estimated Stokes diameter (nm)[a]	estimated MW (kDa)[a]
his-apoE422K empty NLPs	14.2	565
his-apoE422K bR-NLPs	14.8	630
his-apoA1 empty NLPs	10.3	245
his-apoA1 bR-NLPs	10.9	285

[a] Parameters estimated by SEC.

incorporated into a single NLP complex do not necessarily need to be grouped in a trimeric form. The extent of the size variation appears to be governed by the type of NLPs used and might be influenced by lipid displacement (not studied). Calculated MW of apoA1-based particles (Table 1) is in agreement with earlier results where controlled *in vitro* assembly of apoA1-based bR-NLPs complexes were reported[4,22] and correlate well with the apparent MW estimated from native protein acrylamide gel electrophoresis (Figure 2c).

In addition to the bR-NLP complex, the SEC profile also showed a large peak that coeluted with the column's void volume (Figure 2c). This peak, which was also observed in similar experiments where no DNA and no NLPs were included, exhibited no apparent protein content as judged by mass spectrometry analyses (not shown). The above observations suggest that these fractions are composed primarily of non-proteinaceous components that might adsorb to the column's nickel matrix and coelute with the complexes during the affinity purification process.

Height and dispersity of bR-NLP complexes were characterized by AFM, which is a well-established technology previously used to image soluble protein−lipid complexes.[23] Results showed that 80−90% of the particles had a height of approximately 6 nm, which was 1.6 nm larger than empty NLPs and in agreement with the calculated 5 nm height of bR derived from the X-ray structure.[24] These results further support the notion that the complexes are the product of a *bona fide* membrane protein insertion process rather than a consequence of a membrane association or adsorption artifact.

NLPs Must Be Present during the Translation Process. To start to investigate the insertion process mechanism, we performed cell-free reaction assays where NLPs were added before or after peptide chain elongation was inhibited with chloramphenicol (cam). Complex formation and protein activity was observed only when NLPs were added before translation inhibition. Assays where NLPs were added after the addition of cam resulted in inactive bR that did not copurify with NLPs (Figure 3). These observations, together with the fact that under normal reaction conditions the purple color can be observed 5 min after the reaction has started (see above), suggest that the insertion of the MP into the NLP lipid bilayers is part of a cotranslational process.

Further Validation of the Approach. We further validated the method by studying the *in vitro* expression and solubility of a host of MPs of different topologies, sizes, origins, and proposed roles (Figure 4a,b). Sixty-four percent of the proteins analyzed expressed at a level >0.1 mg/mL of the reaction, and without exception, the proteins significantly increased their solubility in the presence of NLPs. For the analyzed data set, the overall solubility increased from 17.3 ± 2.2% to 78.8 ± 3.4%. Remarkably, all the G protein-coupled receptors (GPCRs), despite being notoriously difficult to express in heterologous systems,[1] showed a similar incrrease in solubility when the NLPs were added to the reaction. Recent attempts to express GPCRs *in vitro* relied on reconstitution into liposomes once the protein was synthesized and purified.[25]

In vitro expression in the presence of NLPs produced many MPs at elevated levels that could be readily visualized on a coomassie-stained gel. For example, bR expressed at a rate of 0.9 mg/mL and exhibited virtually 100% solubility when NLPs were added to the reaction (Figure 4c). When DMPC liposomes were included into the reaction, less than 20% of bR remained in the supernatant (not shown), consistent with a previous

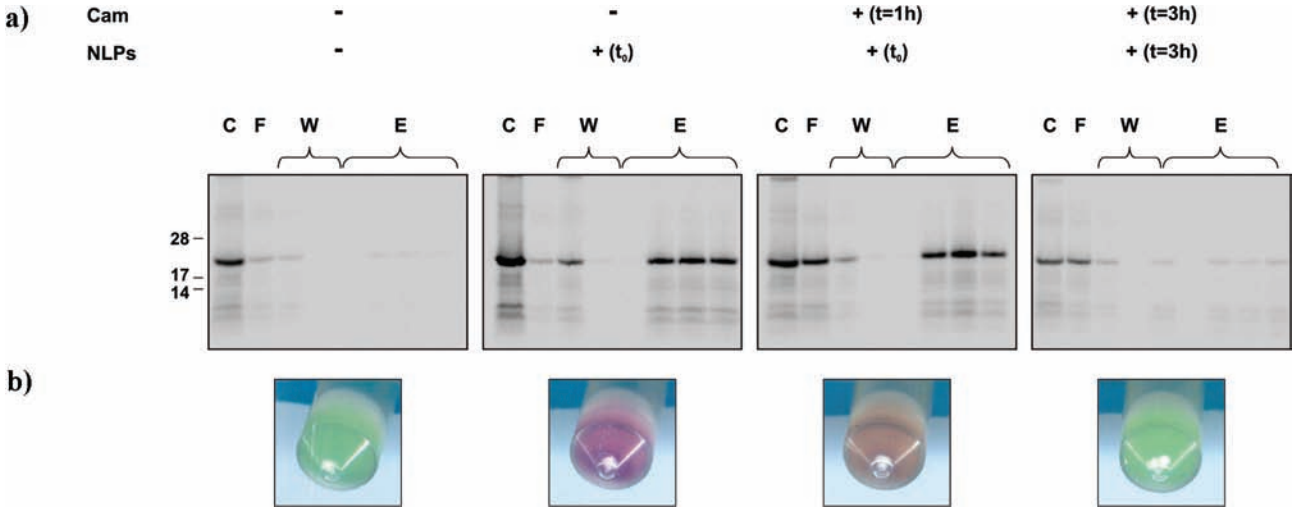

Figure 3. Temporal dependency of membrane protein insertion. (a) bR was expressed *in vitro* in the presence (+) or absence (-) of NLPs. All trans-retinal was added in all cases. Reactions were extended for 4 h. Cam (200 μg/mL) and NLPs were added at the indicated times. When the same time points for both reagents are indicated, cam was added first. NLPs were composed of his-apoA1 as a scaffold and DMPC. Reactions were trace-labeled using [^{35}S]Met. Complexes were purified by nickel-immobilized affinity chromatography, separated by SDS electrophoresis, and visualized by autoradiography. C, crude extract; F, flow-through fraction; W, wash fractions; E, imidazole-eluted fractions. (b) Photograph of the reaction vessels described in panel a. The slightly lighter purple color of the third sample is due to the use of a shorter translation time (1 h) that results in a somewhat reduced amount of bR synthesized.

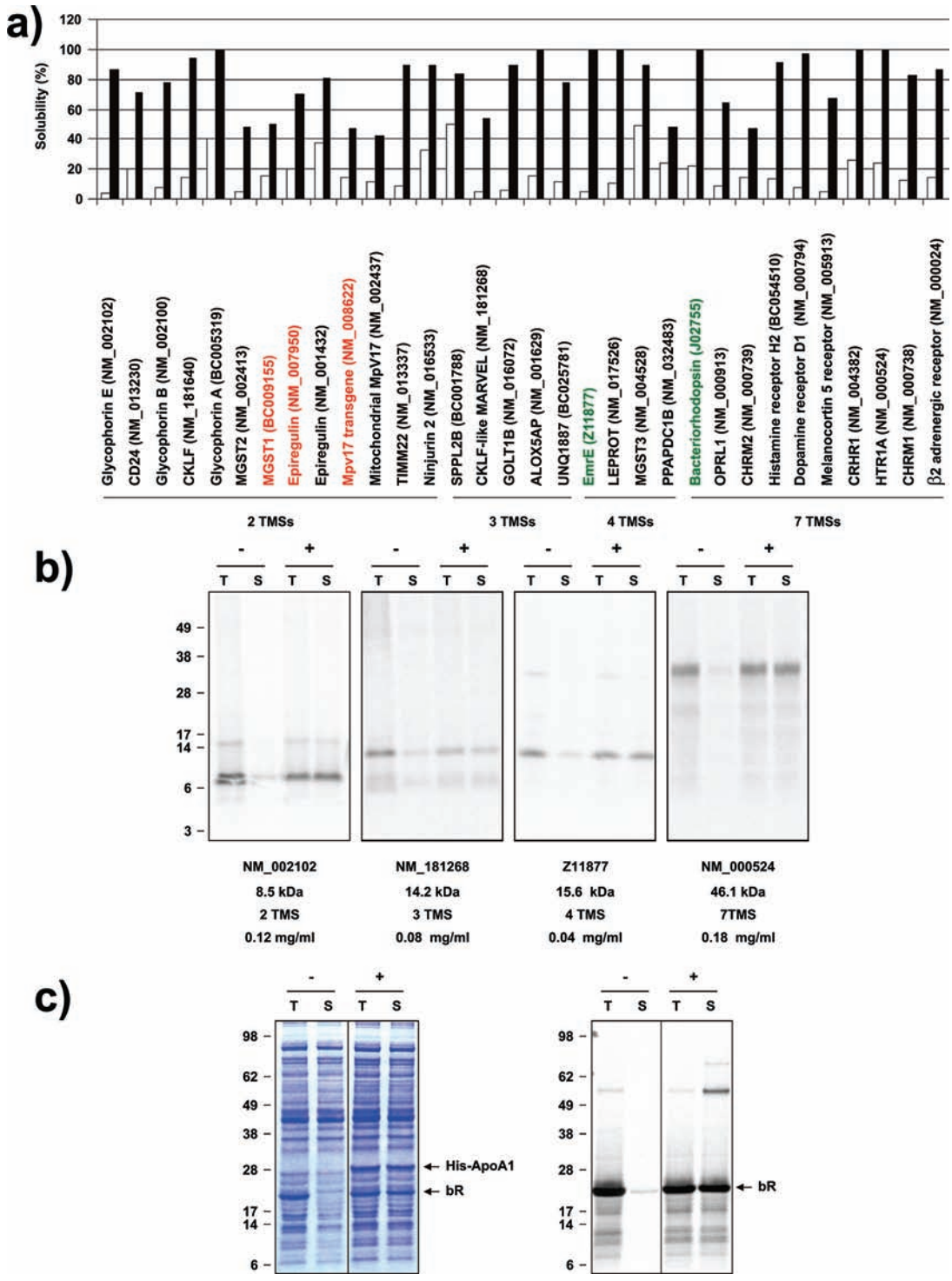

Figure 4. Cell-free expression and analysis of membrane proteins. (a) Thirty-two membrane proteins of human, mouse, and bacterial origin were expressed in the presence (filled bars) or absence (empty bars) of NLPs. NLPs were composed of his-apoA1 as a scaffold and DMPC. Native (nontagged) proteins were expressed from plasmid pEXP4-DEST, with the exception of the product of Z11877 that was expressed from pEXP6-DEST and was tagged with the Lumio epitope. Reactions were trace-labeled using [^{35}S]Met. Annotated gene definitions or gene symbols, GenBank accession numbers, and number of predicted transmembrane segments (TMSs) of their protein products are indicated. Black, red, and green annotations identify the gene source as human, murine, and bacterial, respectively. Protein yield ranged from 0.05 to 0.4 mg/mL of the reaction. (b) Cell-free protein expression samples of a subset of proteins shown in panel a (with the exception of the product of Z11877 that was expressed from pEXP4-DEST) were run on an SDS gel and exposed to an X-ray film. GenBank accession number, predicted MW, predicted number of transmembrane segments, and reaction yield are indicated. (c) Cell-free protein expression samples of bR (GenBank acc. no. J02755) expressed from plasmid pIVEX2.4b in the absence (-) or presence (+) of NLPs, trace-labeled with [^{35}S]Met, run on an SDS gel, stained with coomassie blue (left panel), and exposed to an X-ray film (right panel). bR expressed from this plasmid expresses at a significantly higher level (0.9 mg/mL) than from pEXP4-DEST in panel A (0.4 mg/mL). NLPs were composed of his-apoA1 and DMPC. Corresponding total crude extract (T) and soluble (S) fractions were run on a gel, stained with Coomassie blue, and photographed, and an autoradiogram was prepared.

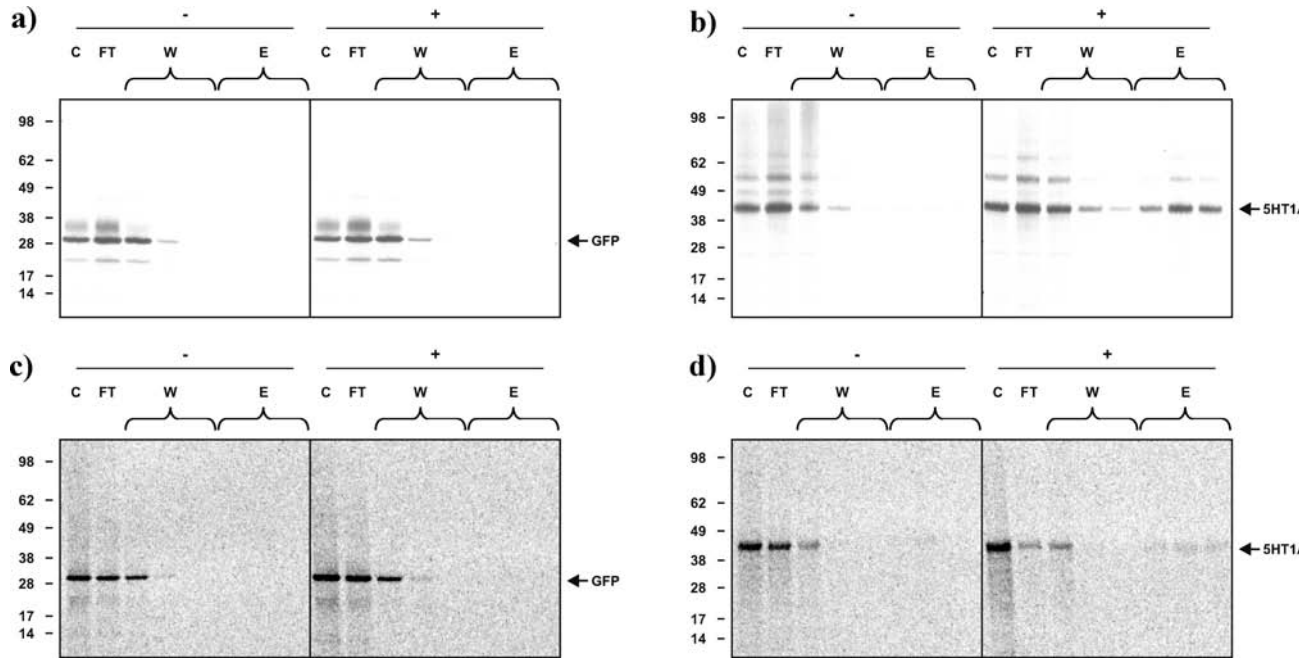

Figure 5. NLP-MP complex formation in eukaryotic cell-free protein expression systems. GFP (a and c) and the human serotonin receptor (5HT1A) (b and d) were expressed and trace-labeled using rabbit reticulocyte (a and b) and wheat germ-based (c and d) cell-free protein expression systems in the presence (+) or absence (-) of NLPs. Proteins, devoid of a histidine tag, were expressed from pFKI032 (GFP) and pEXP4-5HT1A. NLPs were composed of his-apoA1 and DMPC. Complexes were purified by nickel-immobilized affinity chromatography. Proteins were separated by SDS-PAGE and exposed to a film. C, crude extract; FT, flow through fraction; W, wash fractions; E, imidazole-eluted fractions.

report where a small fraction of the translated material where incorporated into the liposomes.[21]

We also evaluated the compatibility of eukaryotic *in vitro* protein expression systems for use with NLPs. Membrane proteins (but not water-soluble proteins such as GFP), readily copurified with histidine-tagged NLP-supplemented rabbit reticulocyte and wheat germ cell-free protein expression reactions (Figure 5), confirming that our approach works not only with prokaryotic, but also with eukaryotic *in vitro* extracts. Although the *E. coli* lysate rendered significantly higher protein yields compared with other lysates (up to 1 mg/mL of the reaction volume), we found that for particularly large eukaryotic membrane proteins (>100 kDa) the bacterial extract produced a small portion of truncated products (for an example, see Supplementary Figure 1).

As opposed to pancreatic dog microsomes, a membrane protein insertion platform developed for the rabbit reticulocyte cell-free protein expression system,[26] NLPs appear to exhibit no detrimental effects on the lysate's translation efficiency (Supplementary Figure 2). Similarly, the use of preparations of enriched *E. coli* membrane vesicles in *E. coli* based cell-free protein synthesis systems has been reported.[27,28] Although this approach demonstrates successful membrane insertion and folding, it relies on a relatively polydisperse and undefined sample and results in products with limited accessibility.

Discussion

We developed a method for the expression and insertion of integral membrane proteins into water soluble discoidal lipoprotein particles. Notable attributes of our approach include (i) unlike conventional membrane protein expression methods, proteins are directly inserted into the final membrane support, avoiding extraction and reconstitution steps; (ii) the process is rapid (from gene to complex under 6 h), flexible (NLP composition can be tailored), high-throughput amenable, compatible with a variety of cell-free lysates, and yields enough product for functional and structural studies; (iii) the protein may be expressed in their native state without the addition of any extraneous sequences; and (iv) the final product is freely accessible from both sides of the lipid bilayer.

Protein insertion into membranes lacking a translocon has been reported previously and the insertion mechanism remains unclear. For example, a number of proteins have been reported to spontaneously integrate *in vitro* into naked liposomes and vesicles.[29–32] Despite significant progress in demonstrating protein insertion and export into and across membranes, the mechanism has been poorly studied at the molecular level. Our novel *in vitro* approach opens new alternatives to study the mechanism of membrane protein insertion and translocation. For example, the strategy sets the basis for recreating *in vitro* the entire membrane protein insertion apparatus by combining a cell-free protein expression system reconstructed from purified components[33] with the recently described bacterial SecYEG translocon assembled into individual disks.[34]

There remain some limitations to our method. First, some membrane proteins appear to need a transmembrane potential for efficient insertion, which in the absence of compartmentalization may not insert appropriately.[35] Second, the intrinsic structure of the discs may exhibit limited flexibility to accommodate particularly large membrane protein complexes. And last, because of their intrinsic folding pathways, some proteins may still need to be subjected to a refolding process once complexed with the NLPs.

Lipid composition of membranes has a profound effect on MP topology and activity.[36] MPs originating from different organisms, tissues, organelles, or even different membrane

domains may require distinct specific environments for proper folding and biological activity. Our system's flexibility in permitting the interchange of NLPs of different chemistries allows the fine-tuning of expression and solubilization conditions for specific MPs to provide near-native context circumventing the biophysical constrains of traditional approaches.

Finally, the method is of special relevance to membrane protein targeting, a developing area of fundamental importance to multiple disciplines including neuroscience, cancer, and developmental biology.

Acknowledgment. We thank Kenneth Rothschild for kindly providing p72bop, Karl Weisgraber for pET32-E4NT, Brent Segelke for providing the E422K protein, Edward Kuhn for making E422K NLPs, Joe Beechem for his insights, Sanjay Vasu for reviewing the manuscript, and Rob Bennett and Claude Benchimol for supporting this project.

Supporting Information Available: Supplementary Figure 1, expression of hERG in *E. coli* and rabbit reticulocyte cell-free protein expression systems; Supplementary Figure 2, effect of NLPs on protein product yield and solubility. This material is available free of charge via the Internet at http://pubs.acs.org.

References

(1) McCusker, E. C.; Bane, S. E.; O'Malley, M. A.; Robinson, A. S. Heterologous GPCR expression: a bottleneck to obtaining crystal structures. *Biotechnol. Prog.* **2007**, *23* (3), 40–47.
(2) Bayburt, T. H.; Carlson, J. W.; Sligar, S. G. Reconstitution and imaging of a membrane protein in a nanometer-size phospholipid bilayer. *J. Struct. Biol.* **1998**, *123* (1), 37–44.
(3) Bayburt, T. H.; Grinkova, Y. V.; Sligar, S. G. Self-assembly of discoidal phospholipid bilayer nanoparticles with membrane scaffold proteins. *Nano Lett.* **2002**, *2* (8), 853–856.
(4) Chromy, B. A.; Arroyo, E.; Blanchette, C. D.; Bench, G.; Benner, H.; Cappuccio, J. A.; Coleman, M. A.; Henderson, P. T.; Hinz, A. K.; Kuhn, E. A.; Pesavento, J. B.; Segelke, B. W.; Sulchek, T. A.; Tarasow, T.; Walsworth, V. L.; Hoeprich, P. D. Different apolipoproteins impact nanolipoprotein particle formation. *J. Am. Chem. Soc.* **2007**, *129* (46), 14348–14354.
(5) Service, R. F. Materials Research Society meeting. Sushi-like discs give inside view of elusive membrane proteins. *Science* **2004**, *304* (5671), 674.
(6) Leitz,A. J.; Bayburt, T. H.; Barnakov, A. N.; Springer, B. A.; Sligar, S. G. Functional reconstitution of Beta2-adrenergic receptors utilizing self-assembling Nanodisc technology. *BioTechniques* **2006**, *40* (5), 601−602, 604, 606, passim.
(7) Sonar, S.; Patel, N.; Fischer, W.; Rothschild, K. J. Cell-free synthesis, functional refolding, and spectroscopic characterization of bacteriorhodopsin, an integral membrane protein. *Biochemistry* **1993**, *32* (50), 13777–13781.
(8) Morrow, J. A.; Arnold, K. S.; Weisgraber, K. H. Functional characterization of apolipoprotein E isoforms overexpressed in Escherichia coli. *Protein Expression Purif.* **1999**, *16* (2), 224–230.
(9) Yerushalmi, H.; Mordoch, S. S.; Schuldiner, S. A single carboxyl mutant of the multidrug transporter EmrE is fully functional. *J. Biol. Chem.* **2001**, *276* (16), 12744–12748.
(10) Sader, J. E.; Larson, I.; Mulvaney, P.; White, L. R. Method for the calibration of atomic force microscope cantilevers. *Rev. Sci. Instrum.* **1995**, *66* (7), 3789–3798.
(11) Elbaz, Y.; Steiner-Mordoch, S.; Danieli, T.; Schuldiner, S. In vitro synthesis of fully functional EmrE, a multidrug transporter, and study of its oligomeric state. *Proc. Natl. Acad. Sci. U.S.A.* **2004**, *101* (6), 1519–1524.
(12) Soskine, M.; Mark, S.; Tayer, N.; Mizrachi, R.; Schuldiner, S. On parallel and antiparallel topology of a homodimeric multidrug transporter. *J. Biol. Chem.* **2006**, *281* (47), 36205–36212.
(13) Sikora, C. W.; Turner, R. J. Investigation of ligand binding to the multidrug resistance protein EmrE by isothermal titration calorimetry. *Biophys. J.* **2005**, *88* (1), 475–482.
(14) Muth, T. R.; Schuldiner, S. A membrane-embedded glutamate is required for ligand binding to the multidrug transporter EmrE. *EMBO J.* **2000**, *19* (2), 234–240.
(15) Tate, C. G.; Ubarretxena-Belandia, I.; Baldwin, J. M. Conformational changes in the multidrug transporter EmrE associated with substrate binding. *J. Mol. Biol.* **2003**, *332* (1), 229–242.
(16) Taylor, E. W.; Agarwal, A. Sequence homology between bacteriorhodopsin and G-protein coupled receptors: exon shuffling or evolution by duplication. *FEBS Lett.* **1993**, *325* (3), 161–166.
(17) Wang, J.; Link, S.; Heyes, C. D.; El-Sayed, M. A. Comparison of the dynamics of the primary events of bacteriorhodopsin in its trimeric and monomeric states. *Biophys. J.* **2002**, *83* (3), 1557–1566.
(18) Mukai, Y.; Kamo, N.; Mitaku, S. Light-induced denaturation of bacteriorhodopsin solubilized by octyl-beta-glucoside. *Protein Eng.* **1999**, *12* (9), 755–759.
(19) Sonar, S.; Lee, C. P.; Coleman, M.; Patel, N.; Liu, X.; Marti, T.; Khorana, H. G.; RajBhandary, U. L.; Rothschild, K. J. Site-directed isotope labelling and FTIR spectroscopy of bacteriorhodopsin. *Nat. Struct. Biol.* **1994**, *1* (8), 512–517.
(20) Popot, J. L.; Gerchman, S. E.; Engelman, D. M. Refolding of bacteriorhodopsin in lipid bilayers. A thermodynamically controlled two-stage process. *J. Mol. Biol.* **1987**, *198* (4), 655–676.
(21) Kalmbach, R.; Chizhov, I.; Schumacher, M. C.; Friedrich, T.; Bamberg, E.; Engelhard, M. Functional cell-free synthesis of a seven helix membrane protein: in situ insertion of bacteriorhodopsin into liposomes. *J. Mol. Biol.* **2007**, *371* (3), 639–648.
(22) Bayburt, T. H.; Grinkova, Y. V.; Sligar, S. G. Assembly of single bacteriorhodopsin trimers in bilayer nanodiscs. *Arch. Biochem. Biophys.* **2006**, *450* (2), 215–222.
(23) Carlson, J. W.; Jonas, A.; Sligar, S. G. Imaging and manipulation of high-density lipoproteins. *Biophys. J.* **1997**, *73* (3), 1184–1189.
(24) Luecke, H.; Schobert, B.; Richter, H. T.; Cartailler, J. P.; Lanyi, J. K. Structural changes in bacteriorhodopsin during ion transport at 2 angstrom resolution. *Science* **1999**, *286* (5438), 255–261.
(25) Klammt, C.; Schwarz, D.; Eifler, N.; Engel, A.; Piehler, J.; Haase, W.; Hahn, S.; Dotsch, V.; Bernhard, F. Cell-free production of G protein-coupled receptors for functional and structural studies. *J. Struct. Biol.* **2007**, *158* (3), 482–493.
(26) Walter, P.; Blobel, G. Preparation of microsomal membranes for cotranslational protein translocation. *Methods Enzymol.* **1983**, *96*, 84–93.
(27) Kuruma, Y.; Nishiyama, K.; Shimizu, Y.; Muller, M.; Ueda, T. Development of a minimal cell-free translation system for the synthesis of presecretory and integral membrane proteins. *Biotechnol. Prog.* **2005**, *21* (4), 1243–1251.
(28) Wuu, J. J; Swartz, J. R. High yield cell-free production of integral membrane proteins without refolding or detergents. *Biochim. Biophys. Acta* **2008**, *1778*, 1237–1250.
(29) Geller, B. L.; Wickner, W. M13 procoat inserts into liposomes in the absence of other membrane proteins. *J. Biol. Chem.* **1985**, *260* (24), 13281–13285.
(30) Klammt, C.; Schwarz, D.; Lohr, F.; Schneider, B.; Dotsch, V.; Bernhard, F. Cell-free expression as an emerging technique for the large scale production of integral membrane protein. *FEBS J.* **2006**, *273* (18), 4141–4153.
(31) Shimizu, Y.; Kuruma, Y.; Ying, B. W.; Umekage, S.; Ueda, T. Cell-free translation systems for protein engineering. *FEBS J.* **2006**, *273* (18), 4133–4140.
(32) Noireaux, V.; Libchaber, A. A vesicle bioreactor as a step toward an artificial cell assembly. *Proc. Natl. Acad. Sci. U.S.A.* **2004**, *101* (51), 17669–17674.
(33) Shimizu, Y.; Inoue, A.; Tomari, Y.; Suzuki, T.; Yokogawa, T.; Nishikawa, K.; Ueda, T. Cell-free translation reconstituted with purified components. *Nat. Biotechnol.* **2001**, *19* (8), 751–755.
(34) Alami, M.; Dalal, K.; Lelj-Garolla, B.; Sligar, S. G.; Duong, F. Nanodiscs unravel the interaction between the SecYEG channel and its cytosolic partner SecA. *EMBO J.* **2007**, *26* (8), 1995–2004.
(35) Andersson, H.; von Heijne, G. Membrane protein topology: effects of delta mu H+ on the translocation of charged residues explain the 'positive inside' rule. *EMBO J.* **1994**, *13* (10), 2267–2272.
(36) Bogdanov, M.; Heacock, P. N.; Dowhan, W. A polytopic membrane protein displays a reversible topology dependent on membrane lipid composition. *Embo J* **2002**, *21* (9), 2107–2116.
(37) Feldman, G.; Bogoev, R.; Shevirov, J.; Sartiel, A.; Margalit, I. Detection of tetracysteine-tagged proteins using a biarsenical fluorescein derivative through dry microplate array gel electrophoresis. *Electrophoresis* **2004**, *25* (15), 2447–2451.

PR800265F